2023-03-10

Sources of Atmospheric Dust Deposition on Utah Lake

Justin Telfer
Brigham Young University

Sources of Atmospheric Dust Deposition on Utah Lake

Justin Telfer

A thesis submitted to the faculty of
Brigham Young University
in partial fulfillment of the requirements for the degree of

Master of Science

Gustavious P. Williams, Chair
A. Woodruff Miller
Robert Sowby

Department of Civil and Construction Engineering

Brigham Young University

Abstract

Atmospheric deposition (AD) is a significant source of nutrient loading to waterbodies around the world. However, the sources and loading rates are poorly understood for major waterbodies and even less understood for local waterbodies. Utah Lake is a eutrophic lake located in central Utah, USA, and has high nutrient levels. Recent research has identified AD as significant sources for nutrient loading to the lake to better understand the dust AD sources, we sampled suspected source locations and collected deposition samples around the lake. We analyzed these samples using Inductively Coupled Plasma (ICP) for 25 metals to characterize their elemental fingerprints. We then compared the lake samples to the source samples to determine likely source locations. We computed spectral angle, coefficient of determination, multi-dimensional scaling, and radar-plots to characterize the similarity of the samples. We found that lake deposition samples were more similar to local sources than to distant sources. This suggests that the major source of atmospheric deposition onto Utah Lake is the local empty fields south and west of the lake and not the farther playa sources as previously suggested. Preliminary data suggest that dust AD is associated with dry, windy conditions and is episodic in nature. We show that AD from dust deposition is likely a small portion of the overall AD nutrient loading on Utah Lake, with the dry and precipitation source contributing the majority of the load.

Keywords: atmospheric deposition; nutrient loading; Utah Lake

Acknowledgments

I would like to thank Dr. Gustavious Williams, Wood Miller, and Rob Sowby for allowing me to work as a grad student under them. For the help and tutelage, they each patiently provided me; To Dr. Theron Miller for allowing me to use his equipment and provide expertise, as well as the project idea; To the Wasatch Front Water Quality Council for funding this project; To Erin Jones and the BYU Environmental Analytic Lab for the training and equipment to perform the needed testing; To Mitch Brown for all his help collecting the samples; and to my loving wife who patiently gave me encouragement even when I was stressed and cranky.

Table of Contents

List of Figures

List of Tables

1 Introduction

Utah Lake is a large but shallow eutrophic freshwater lake located in the center of Utah county. The lake has large population centers on the north and east sides that potentially increase nutrient pollution loadings to the lake. While the south and west sides of the lake are not yet densely populated, they are being developed and will likely continue to grow in the future. The lake is classified as hyper-eutrophic by the Larsen-Mercier Trophic State model but only moderately eutrophic by the Carlson Trophic State Index [1]. The lake has a surface area of roughly 375 km2 (~92,665 acres) but an average depth of only 3 m (~10 ft) during non-drought years and even shallower during drought years [2]. The shallow depths create a surface-area-to-volume ratio that makes the lake more susceptible to nutrient deposition from the atmosphere than deeper lakes [2, 3]. While nutrients like nitrogen and phosphorus are often the limiting factor in aquatic plant growth [4], Utah Lake plant growth may be limited by high turbidity causing reduced light penetration [1]. However, recent studies have shown that algal blooms, as measured by remote sensing methods, show no trends over the last 40 years [5-7].

Atmospheric deposition of nitrogen can occur through dry (includes gaseous), dust, and bulk (precipitation) deposition. Unlike nitrogen, phosphorus does not have a stable gaseous phase, but is often associated with particles <2.5 μm, and larger dust particles. So even though phosphorous does not have a gas phase, dry, dust, and bulk (precipitation) AD deposition associated with particulates occurs [8]. Many human activities including combustion, mining, agriculture, and transportation increase particulate dust generation, and therefore atmospheric deposition [8]. In recent history dust generation has increased due to anthropogenic activities and climate change [9, 10], with one study estimating that over the last 100 years 40% more dust has been put into the atmosphere due to anthropogenic activity [11]. Some anthropogenic activities, like agriculture, not only increase dust production [12] but can increase nutrient levels, especially during planting and fertilization [13]. Human diversions of water have combined with climate change to cause lakes around the world to dry up, exposing lakebeds that further increase mineral dust generation [14-17].

The way particulates settle in the atmosphere depends on their size and weight. Larger particulates tend to settle to the ground faster than smaller particulates [18]. Hinds and Zhu [18] state that particle size is the most important parameter for characterizing aerosol behavior. They show that particles with equivalent diameters of 0.1, 1.0, 10, and 100 μm settle in perfectly calm air at 8.8x10-7, 3.7x10-5, and 3.1x10-3, and 2.5x10-1 meters per second (m/s), respectively. This means that for particles smaller than about 10 μm a light breeze can keep the particle from settling. Particulates such as photochemical smog (mostly nitrogen particles), smokes, and fine dust less than 2.5 μm essentially do not settle from the atmosphere, but are kept aloft by Brownian motion and wind currents [18]. Particles in the poorly settling 0.2-10 micron range are often enriched in phosphorus, leading to higher nutrient deposition when that fraction is involved [19].

For discussion purposes we break AD into three categories: dust, dry, and bulk (precipitation). We define dust as particles larger than ~2.5 μm and generally settle, dry as particles less than ~2.5 μm that are less apt to settle but are removed by contact, and bulk (precipitation) any nutrients deposit with precipitation which includes both dry, dust, and any gases or smaller particles in the atmosphere. Nutrients related to dry deposition and the small particle fraction of precipitation deposition can travel long distances and can be difficult to attribute to a specific source. Dust particles (> 2.5 μm) settle out of the atmosphere and subsequently do not often travel as far. AD from dust can be associated with high wind events or activities that mobilize dust from the surface.

Recently interest in the nutrient loadings to Utah Lake has grown significantly as the Utah Division of Water Quality (DWQ) looks to reduce wastewater treatment plant phosphorus discharge limits to 0.1 mg/L [2]. It is estimated that these reductions could cost up to 1 billion dollars statewide to fully achieve [2]. However, it is not clear that the algal blooms are directly caused by the wastewater treatment plant nutrients. Some evidence suggests the algal blooms are not related to wastewater plants and that the algal blooms have slightly decreased over the last 40 years [5]. Abu-Hmeidan, Williams [20] have shown that phosphorus levels in ancient Utah Lake sediments are not statistically different from current sediments, suggesting that the historically recent wastewater plants are not causing nutrient increases in the lakebed [20]. The lake has been shown to retain 90 percent of phosphorus loadings, likely stored in the sediments, further supporting a historical phosphorus buildup [1].

Several past studies, including research done by DWQ, have looked at nutrient loadings to the lake through natural water inflows and wastewater treatment effluents and found high nutrient loads [1]. The studies, however, failed to consider atmospheric deposition or geologic conditions as a significant source of nutrients, likely due to limited available information [21]. More recent studies have shown that atmospheric deposition is indeed a major contributor of both phosphorus and nitrogen to waterbodies and even suggest that atmospheric deposition alone could keep Utah Lake eutrophic [3, 11, 21-25]. Research looking at sediment nutrients have found them to be a significant source even without external loadings, providing as much as 19 mg/L of phosphorus to laboratory water column samples [20]. The geologic nature of the area also supports historically high phosphorus levels, as the Utah Lake watershed contains a major phosphorus deposit [26].

The research focusing on Utah Lake deposition specifically have focused on different methods of deposition. Unpublished studies by Dr. A. Woodruff Miller at Brigham Young University have focused on bulk deposition only and estimate that 100 tons/year of total phosphorus falls on Utah Lake. Unpublished works by Brahney [8] and Carling for the Utah Lake Science Panel have focused on dry deposition only and estimate between 4 and 13 tons/year of total phosphorus. Barrus, Williams [21] looked at total deposition producing estimates between 130 and 260 tons/year of total phosphorus deposition [21]. When adding the dry and bulk estimates from Brahney [8] and Miller respectively, we get results similar to Barrus, Williams [21]; however, the groups cannot agree on each other's methods.

Research by Carling, Fernandez [27] looked at sources and composition of atmospheric deposition onto the Wasatch Front, not specifically Utah Lake, finding distant desert playas in southwest Utah to be the main source of deposition [27, 28], with dust being transported by southern winds funneled by area geography. However, these studies focused on larger wind events that average only 4.3–4.7 events per year, used deposition sampler designs that discriminate against local sources, and never tested the samples against local areas. While Carling, Fernandez [27] found distant desert playas to be the source other works have shown proximal sources to be an underrepresented source[29]. We extend this work by testing both local and distant sources.

This paper aims to provide further understanding of the sources and composition of atmospheric deposition onto Utah Lake. We hypothesize that smaller, local storms are transporting local soils near the lake in smaller quantities but much more frequently. We test this hypothesis by comparing elemental fingerprints of dust samples we collected near the lake to samples collected from possible source locations.

2 Materials and Methods

2.1 Utah Lake Deposition Sample Collection

To characterize atmospheric deposition on Utah Lake, five sampler sites were chosen surrounding the lake and according to National Atmospheric Deposition Program (NADP) protocols [30]. The sampler design, seen in Figure 1, consisted of a dry deposition bucket with 3-4 liters of water and an empty wet deposition bucket with a lid moving to cover one side at a time. The samplers were already placed, locations in shown in Figure 2, and being used for deposition research requiring a small portion of the sample for separate testing. The operation, maintenance, and sampling procedures were done in accordance with the design of previous studies [3, 21]. We collected samples weekly, when possible, from May to October of 2022 and combined them into a spring sample (May–July) and a fall sample (August–October).

Figure 1. Atmospheric deposition samplers designed to collect wet and dry deposition in separate buckets with a moving lid mechanism.

Due to the samplers being used for separate research, we first had to decant 300-400 mL of sample for separate testing with the remainder used for our study. However, wet deposition samples rarely contained more than 300-400 ml, so no wet deposition was available for our study.

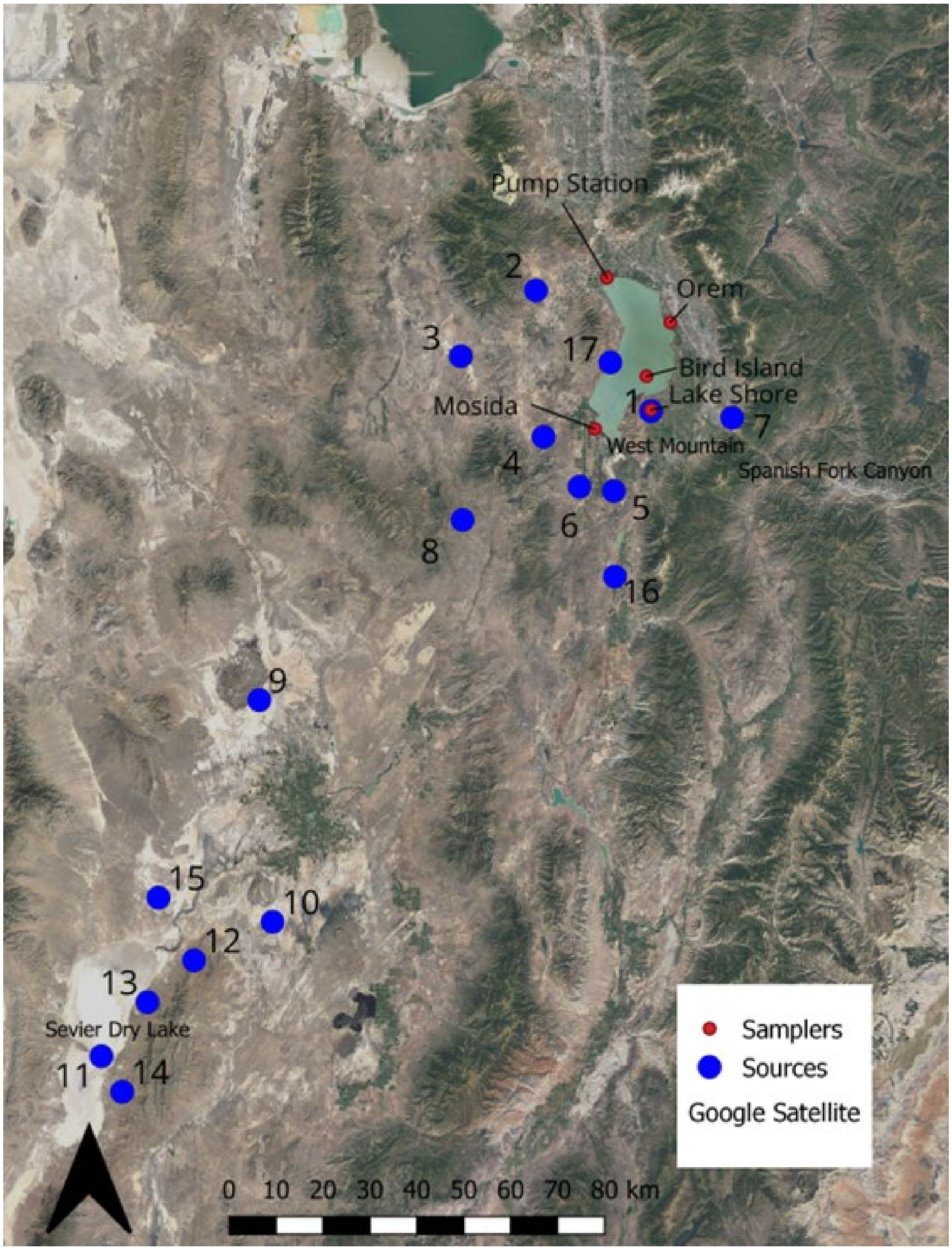

Figure 2. Samplers were placed around Utah Lake with one sampler on Bird Island. The dust source locations were chosen at the southern half of Utah Lake and in a southwest direction towards Sevier Dry Lake. Source numbers: 1=Lake Shore, 2=Eagle Mountain, 3=5-Mile Pass, 4=Chimney Rock Pass, 5=Goshen WMA, 6=Elberta, 7==Mouth of Spanish Fork Canyon, 8=Cherry Creek, 9=Fumarole Butte, 10=Sunstone Knoll, 11=Sevier Dry Lake, 12= Cricket Mountain, 13=White Hills near Sevier Lake, 14=Mid-Sevier Lake near road, 15=Highway 6 South of Delta, 16=Burraston Ponds, and 17=Miners Canyon.

2.2 Source Dust Sample Collection

We collected source dust samples in open areas between Sevier Dry Lake and Utah Lake, as well as in suspected sources surrounding the lake as shown in Figure 2. While previous testing by Goodman, Carling [28] and Carling, Fernandez [27] tested only southwestern playa sources, a wind rose showing winds since 1980 for the Provo Airport suggest winds originating from the southeast, likely Spanish Fork Canyon, are reaching the east side of the lake. To test this, we collected a source dust sample at a construction site near the mouth of the canyon where active dust transport was witnessed. In total 17 dust samples were collected with 3 at the same locations as Goodman, Carling [28] including Sevier Dry Lake, Sunstone Knoll, and Fumarole Butte. The Provo Municipal Wind Rose and the wind path from Spanish Fork Canyon are seen in Figure 3.

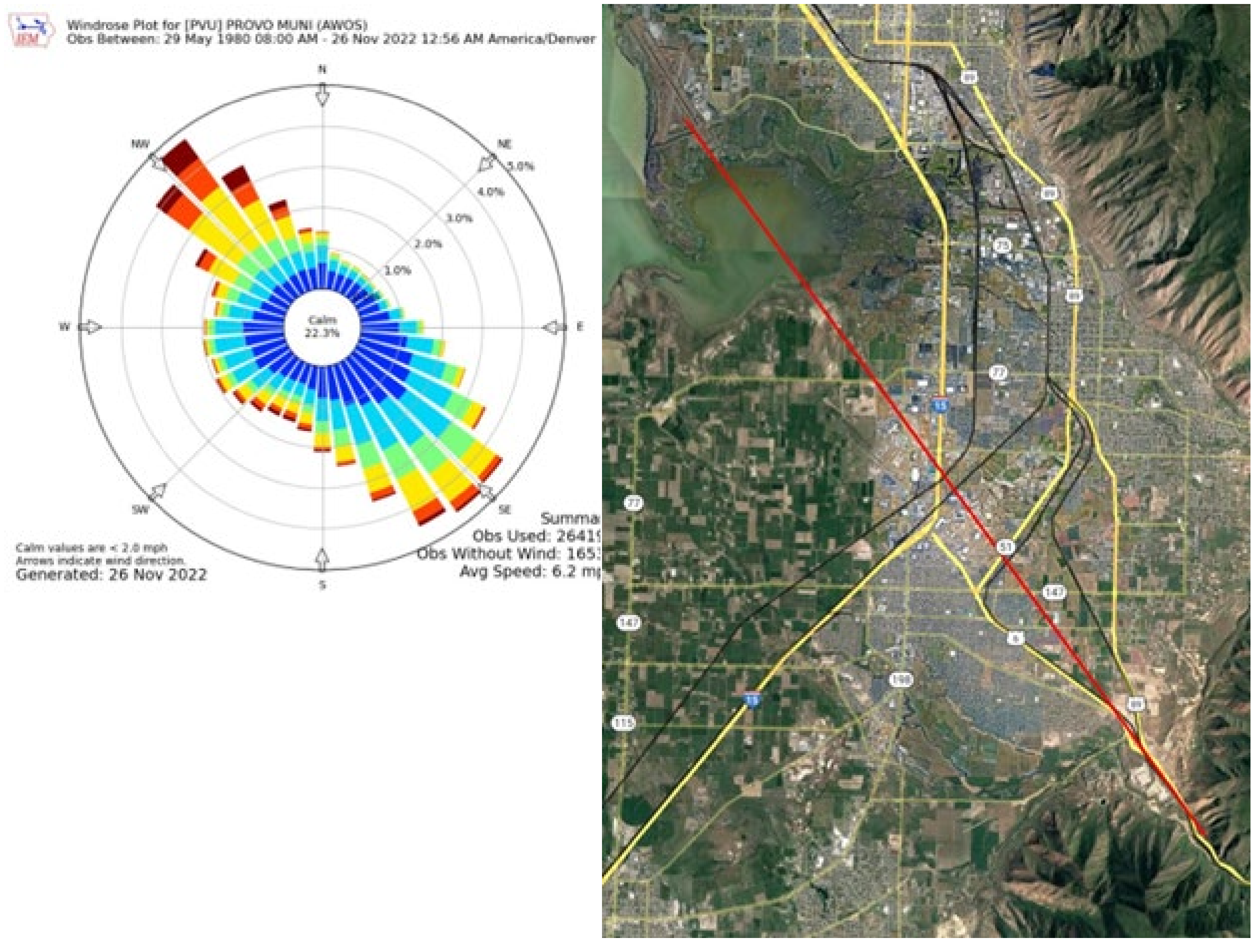

Figure 3. Historic wind rose since 1980 for the Provo Municipal Airport suggesting a wind path from the mouth of Spanish Fork Canyon

Soils from these locations were collected in accordance with EPA AP-42 Appendix C-1 procedures as done in previous dust studies [31, 32]. Soils were scraped with a shovel in an upward direction to a depth of ~2.5 cm (1 inch) or the diameter of the largest particle, whichever was less. As recommended by the EPA, all particles in the area were collected and large particles were not avoided. The EPA recommends collecting 10 pounds per site, but we only collected 1-2 pounds to allow for easier storage and transport.

2.3 Sample Preparation and Analysis

We first sieved the source dust samples with a 250-micron sieve for 5 minutes to remove large particles unlikely to be transported by wind. This sieve size was chosen based on previous particle size analysis done by Dansie, Wiggs [33], Chepil [34], and Péwé [35] to eliminate particles too large to travel the needed distances. The source dust samples were not treated in any way to remove organics as organics passing through the sieve were small enough to be transported with the dust. The Sevier Dry Lake sample was collected wet and allowed to dry naturally over time; this caused the sample to dry into hard clumps that were not easily broken. These clumps were broken apart using a soil flail grinder. Six of the source dust samples were collected when damp and dried in a drying chamber at 45 degrees Celsius overnight. This drying procedure caused some small clumping of the samples, and the clumps were gently broken down using a clean spatula before sieving.

We filtered the lake deposition samples through a 0.45-micron cellulose acetate vacuum filter to separate particulates from water. This filter type was chosen to allow separation of the sample from the water without affecting the nitric acid digestion and ICP-OES analysis. Other separation techniques and filter types were attempted with little success. The last sample from the pump station sampler collected on October 10th had heavy contamination from the seal material on our sampler's lid. This sample, labeled pump station contamination or PS contamination, was processed separately from the other pump station samples but did not show a significant difference in the end. The cellulose acetate filters are extremely low ash content, and the filters with sample were put in a muffle furnace at 500 degrees Celsius for 2.5 hours to remove the filter from the samples [36].

After being filtered or sieved the resulting samples were digested using a nitric acid microwave digestion. This digestion used 69.9% nitric acid at 170 degrees Celsius for 20 minutes with 50 minutes of warmup and cooldown time.

The samples were then analyzed for element concentrations on a Thermo-Scientific iCAP7400 Radial ICP-OES. Concentrations were measured for Al, As, B, Ba, Ca, Cd, Co, Cr, Cu, Fe, K, Mg, Mn, Mo, Na, Ni, P, Pb, S, Se, Si, Sr, Ti, V, and Zn. The elements Cadmium and Selenium were below detection limits for all samples except 2 mg/kg Selenium at Goshen WMA, so they were removed from the analysis. The detection limits were calculated according to the EPA method detection limit procedure, and the standard used was the BYU Environmental Analytic Lab soil standard.

2.4 Data Analysis

A simple Python script was created to compare the lake deposition samples to the source dust samples using spectral angle, and coefficient of determination (R2). Spectral angles are the angles created between two dissimilar vectors. We created vectors for our samples by assigning each analyzed value a point in an n-dimensional space, where n is the number of values. For this approach we assume each metal concentration is a separate dimension. The angle between these vectors is then measured and low spectral angles were considered similar samples. Using spectral angles allows us to compare datasets for similar ratios between elements so that magnitude differences do not interfere. This technique has been used to find similarities between geologic samples in previous studies [37]. We used a spectral angle script found in the Python hydrostats library. **[38]**.

Multidimensional scaling was performed in SAS JMP Pro. Multi-Dimensional Scaling (MDS) is a form of non-linear dimensionality reduction that allows visualization of similarity between samples, generally in a 2-dimensional plot. An MDS plot is interpreted by comparing the proximity of samples, with similar samples placed close together and dissimilar samples spread apart. This technique has previously been used to interpret similarities in geologic samples [39, 40]. SAS JMP Pro was also used to create a Shepard Diagram and stress value for our results. Shepard Diagrams and stress values are used to determine the goodness-of-fit for the MDS plot. The Shepard Diagram provides a coefficient of determination value, and the stress value is from 0-1 with small values being a better fit.

Radar Diagrams were created from our data using a custom python script. Radar plots allow for quick visualization of the similarities and differences between the samples without any form of analysis. Our raw uncorrected ICP results were used for the radar plots because the dilution-corrected results created a large difference in magnitudes unable to fit on a single plot. The calcium values also were corrected by a factor of 12 to fit the radar diagram scale. When using radar plots the magnitude is insignificant; the ratios between elements, and the shape they create, are what was analyzed.

3 Results

3.1 Spectral Angle and Coefficient of Determination

We found high similarity, or low spectral angles, between the Cherry Creek source sample and the lake deposition samples. The Lake Shore deposition was the least related. The source sample from Chimney Rock Pass is the second closest source sample. The results of the spectral angle script are seen in the heat map in Figure 4 with darker reds, meaning lower angles, being the most similar. Cherry Creek is seen near the top of the map with a dark horizontal line denoting low spectral angles between samples. The Mosida fall deposition sample was closest to Cherry Creek with the two lines differing by only 0.34 radians. When considering the geography of the Cherry Creek area, winds from the southwest are funneled to the Mosida sampler first before opening and diluting into Utah valley. The least similar deposition samples to Cherry Creek are the two Lake Shore samples with the two lines differing by 0.79 and 0.67 radians. This is again explained with local geography as the path between the two locations is blocked by West Mountain. Analyzing the same dataset using a simple coefficient of determination analyses shows comparable results to spectral angles shown in the heatmap in Figure 5.

Spectral Angle Comparison	Samples									
Sources	Mosida Fall	Orem Fall	Lake Shore Fall	Pump Station Fall	Mosida Spring	Orem Spring	Lake Shore Spring	Pump Station Spring	Bird Island All	PS contaminated
5-mile Pass	0.72	0.94	0.86	0.73	1.02	1.04	1.07	0.91	1.06	0.78
Burraston Ponds	0.69	0.91	0.86	0.70	0.98	1.01	1.06	0.88	1.03	0.74
Cherry Creek	0.34	0.54	0.67	0.35	0.60	0.63	0.79	0.51	0.65	0.38
Chimney Rock Pass	0.49	0.70	0.74	0.50	0.77	0.79	0.90	0.66	0.81	0.54
Cricket Mountain	0.87	1.08	0.97	0.88	1.16	1.18	1.19	1.06	1.21	0.92
Eagle Mountain	0.66	0.88	0.85	0.67	0.95	0.98	1.05	0.85	1.00	0.72
Elberta	0.60	0.81	0.81	0.61	0.88	0.90	0.99	0.77	0.93	0.65
Fumerole Butte	0.83	1.03	0.89	0.84	1.11	1.13	1.10	1.02	1.17	0.88
Goshen WMA	0.90	1.11	0.94	0.91	1.19	1.21	1.17	1.09	1.24	0.95
Hwy 6 South of Delta	0.93	1.15	1.04	0.94	1.23	1.25	1.26	1.12	1.27	0.99
Lake Shore	0.78	0.96	0.68	0.79	1.06	1.07	0.92	0.99	1.12	0.82
Mid Sevier Lake by road	0.81	1.03	0.94	0.82	1.11	1.13	1.16	1.00	1.15	0.87
Miners Canyon(W. Utah Lake)	0.65	0.86	0.82	0.66	0.94	0.96	1.02	0.83	0.98	0.70
Mouth S.F. Canyon	0.65	0.86	0.82	0.66	0.94	0.96	1.02	0.83	0.99	0.70
Sevier Lake	0.89	1.05	0.86	0.89	1.12	1.13	1.05	1.05	1.17	0.93
Sunstone Knoll	0.84	1.04	0.96	0.84	1.11	1.14	1.16	1.01	1.16	0.89
White Hills Sevier Lake	0.90	1.11	1.01	0.91	1.19	1.21	1.22	1.08	1.24	0.95

Scale	
0.08	Better Fit
0.15	
0.23	
0.31	
0.38	
0.46	
0.53	
0.61	
0.69	
0.76	
0.84	
0.92	
0.99	
1.07	
1.14	
1.22	
1.30	Poor Fit

Figure 4. Heatmap showing the results of spectral angle analysis comparing sources (vertical) to deposition (horizontal) samples. Darker reds represent more similarity and Cherry Creek is the closest to all the samples. The sample that Cherry Creek is farthest from is the Lake Shore spring sample with the two lines differing by 0.79 radians.

Coefficient of Determination Comparison	Samples											
Sources	Mosida Fall	Orem Fall	Lake Shore Fall	Pump Station Fall	Mosida Spring	Orem Spring	Lake Shore Spring	Pump Station Spring	Bird Island All	PS contaminated	Scale	
5-mile Pass	0.68	0.53	0.61	0.68	0.46	0.46	0.44	0.55	0.43	0.65	1.00	Good Fit
Burraston Ponds	0.72	0.57	0.63	0.72	0.51	0.50	0.47	0.59	0.48	0.69	0.94	
Cherry Creek	0.93	0.86	0.79	0.94	0.82	0.81	0.72	0.87	0.80	0.92	0.88	
Chimney Rock Pass	0.85	0.73	0.72	0.85	0.68	0.68	0.60	0.76	0.65	0.83	0.81	
Cricket Mountain	0.53	0.35	0.47	0.53	0.28	0.27	0.27	0.37	0.24	0.49	0.75	
Eagle Mountain	0.74	0.60	0.64	0.75	0.54	0.53	0.48	0.62	0.50	0.72	0.69	
Elberta	0.77	0.64	0.66	0.77	0.58	0.57	0.51	0.66	0.54	0.75	0.63	
Fumerole Butte	0.54	0.38	0.53	0.55	0.31	0.30	0.34	0.39	0.26	0.51	0.56	
Goshen WMA	0.47	0.30	0.47	0.48	0.22	0.22	0.27	0.31	0.18	0.44	0.50	
Hwy 6 South of Delta	0.46	0.28	0.40	0.47	0.20	0.20	0.20	0.30	0.16	0.42	0.44	
Lake Shore	0.61	0.47	0.70	0.60	0.39	0.39	0.52	0.46	0.34	0.58	0.38	
Mid Sevier Lake by road	0.58	0.42	0.51	0.59	0.35	0.34	0.32	0.44	0.31	0.55	0.31	
Miners Canyon(W. Utah Lake)	0.73	0.59	0.64	0.74	0.53	0.52	0.48	0.61	0.49	0.71	0.25	
Mouth S.F. Canyon	0.72	0.58	0.63	0.73	0.51	0.51	0.47	0.60	0.48	0.70	0.19	
Sevier Lake	0.48	0.36	0.54	0.50	0.29	0.29	0.38	0.36	0.25	0.46	0.13	
Sunstone Knoll	0.54	0.38	0.47	0.55	0.31	0.30	0.29	0.40	0.27	0.51	0.06	
White Hills Sevier Lake	0.49	0.31	0.43	0.50	0.24	0.23	0.23	0.34	0.20	0.45	0.00	Poor Fit

Figure 5. Heatmap showing the results of coefficient of determination analysis. The darker red colors show a closer relation and again Cherry Creek is the most similar to all samples collected. The lowest relation is again the Lake Shore spring sample with only 72% of the variation explained.

3.2 3.Multi-Dimensional Scaling Comparison

The SAS JMP Pro results show that several local source samples cluster closely with the lake deposition samples. As seen in the MDS plot in Figure 6, samples to the west of Utah Lake, including Cherry Creek, Miners Canyon, Elberta, and Chimney Rock Pass, and the mouth of Spanish Fork Canyon on the east side, are the closest to the lake samples. This result is comparable to the spectral angle and R2 comparison in Figures 4 and 5.

Also seen in Figure 6, similar to the spectral angle comparison, is the two Lake Shore deposition samples being the least similar to the local sources. This is again explained by the Lake Shore sampler being at the base of the West Mountain, blocking transport from local sources. An interesting result is that while the two Lake Shore samples are not clumped with the local sources to the southwest, like the other samples, they are also not grouped near sources collected directly south of the sampler. The Lake Shore dust source sample was collected directly south of the Lake Shore sampler yet still shows low proximity to the lake deposition sample. This may suggest that the main source of the Lake Shore deposition is still from southwest but originating in West Mountain itself, which was not tested in this study. The Lake Shore sampler also shows the closest proximity to the Sevier Dry Lake sample, suggesting that the West Mountains are blocking local transport, but not long-range transport.

Another interesting result shown in Figure 6 is the similarity between Mosida, Bird Island, and Orem, this is seen by how close the points are located. Previous criticisms of deposition research done by Barrus, Williams [21] claimed that deposition should differ between shoreline samples and mid-lake samples. The Orem Deposition sample is grouped with the Mosida and Bird Island samples suggesting that the source of lake deposition is the same for all three samplers. Because Bird Island is in the middle of the lake and Orem is on the far side from Mosida, this result supports Barrus, Williams [21] claims of little difference in shoreline to mid-lake sediment deposition.

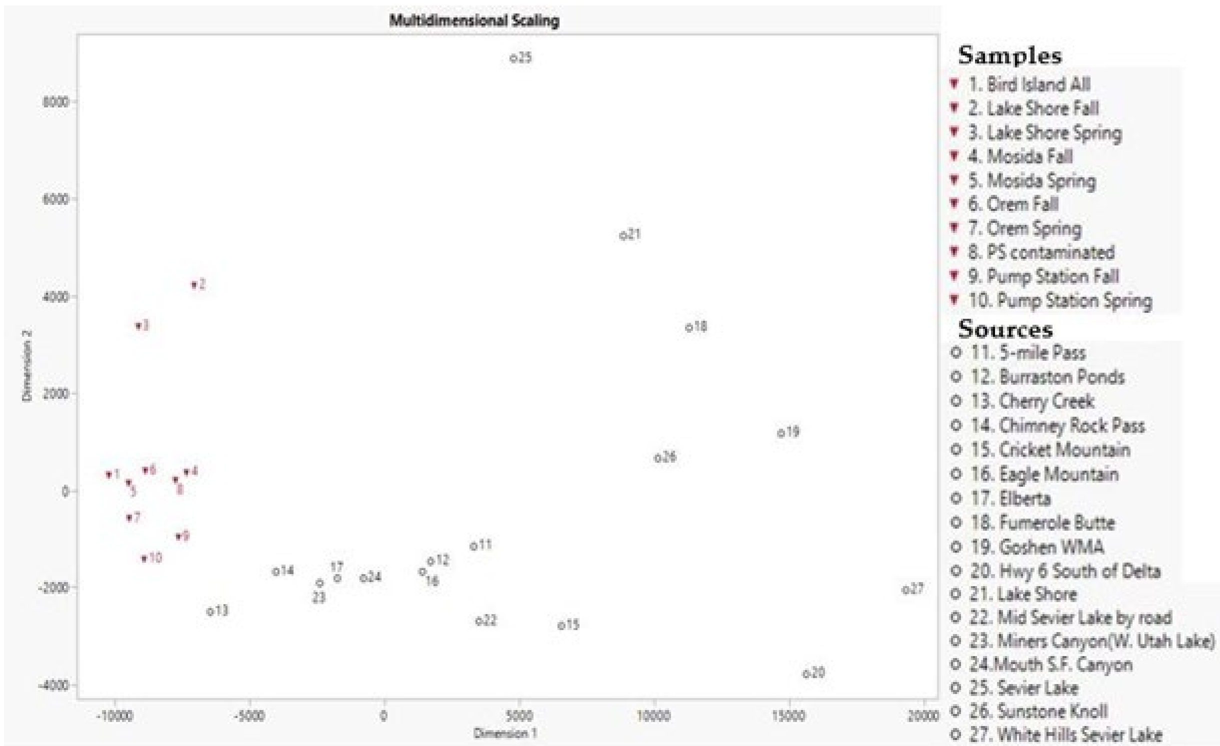

Figure 6. Multi-Dimensional Scaling (MDS) plots place similar samples close together and less similar farther apart. Our MDS shows a strong similarity between deposition samples, excluding the two Lake Shore samples, and local sources, with Cherry Creek and Chimney Rock Pass the most similar. The distant playa samples are not grouped with the deposition sources, although the two Lake Shore samples are closest to several of the playas.

The JMP Shepard diagram for our MDS plot allows quick determination of the plot's accuracy. Shepard diagrams show how well the MDS plot reflects the actual vs. the predicted proximities of the samples. The Shepard diagram for our MDS plot is seen in Figure 7 and shows a strong fit for the data with an R2 value of 0.993. JMP also provides a stress value for the MDS plot. Stress values are a goodness of fit measure showing the degree of correspondence between values and range from 0-1, with smaller stress values indicating a better fit. JMP uses a Kruskal Stress equation that gives a stress value of 0.047 signifying a good fit [41].

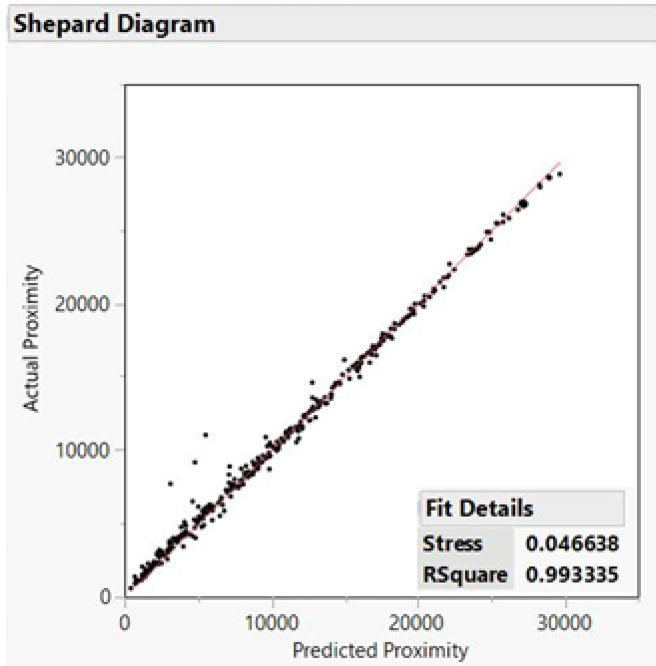

Figure 7. Shepard diagram for the MDS plot showing a strong fit for predicted vs actual locations. The R2 value for the Shepard diagram is 0.99 and the stress value is 0.05 supporting a strong fit.

3.3 Radar Plot Visual Comparison

As seen in Figure 8, Cherry Creek is visually similar to both the Mosida fall and Orem fall samples, but different compared to the Sevier Dry Lake sample. Looking at the Cherry Creek sample compared to the lake deposition samples the only large difference is Cherry Creek's high silica and calcium concentrations. This could be due to using too large a sieve allowing silica grains to pass that would not have been transported by wind. We sieved the Cherry Creek sample with a 150-micron screen to test this but found no major difference. The likely cause is inefficient wind transport of silicates compared to the other elements [8]. The similarity between Mosida and Orem also shows that the sources of the dust are likely the same, supporting the claims that dust deposition across the lake is does not change significantly.

Figure 8. Similarity between the (a) Mosida fall and (b) Orem fall samples is easily seen using radar plots. The (c) Cherry Creek sample has more silica and calcium than the deposition samples, ignoring silica the similarity is easy to see. Also easy to see are the differences between the first three and (d) Sevier Dry Lake.

3.4 Low Levels of Dust Deposition

Members of the Utah Lake Science Panel have argued that the main source of nutrient loading to Utah Lake is dust. Using the nutrient levels measured in sediments surrounding Utah Lake, they estimated an impossible amount of dust deposition is required to get the nutrient loadings calculated by Barrus, Williams [21]. While the purpose of this study wasn't to measure dust falling on the lake, we did measure what was collected for the ICP analysis. The weight of dust collected for the 5.5 months of this study, seen in Table 1, show very small amounts collected. Several of the weeks during this study had samples with algae growing in the buckets, this would have clogged the membrane filters, so the samples were not used. This means that the dust collected is not truly representative of the amount falling on the lake. However, the samples discarded are unlikely to have raised the collection amount significantly.

(a)

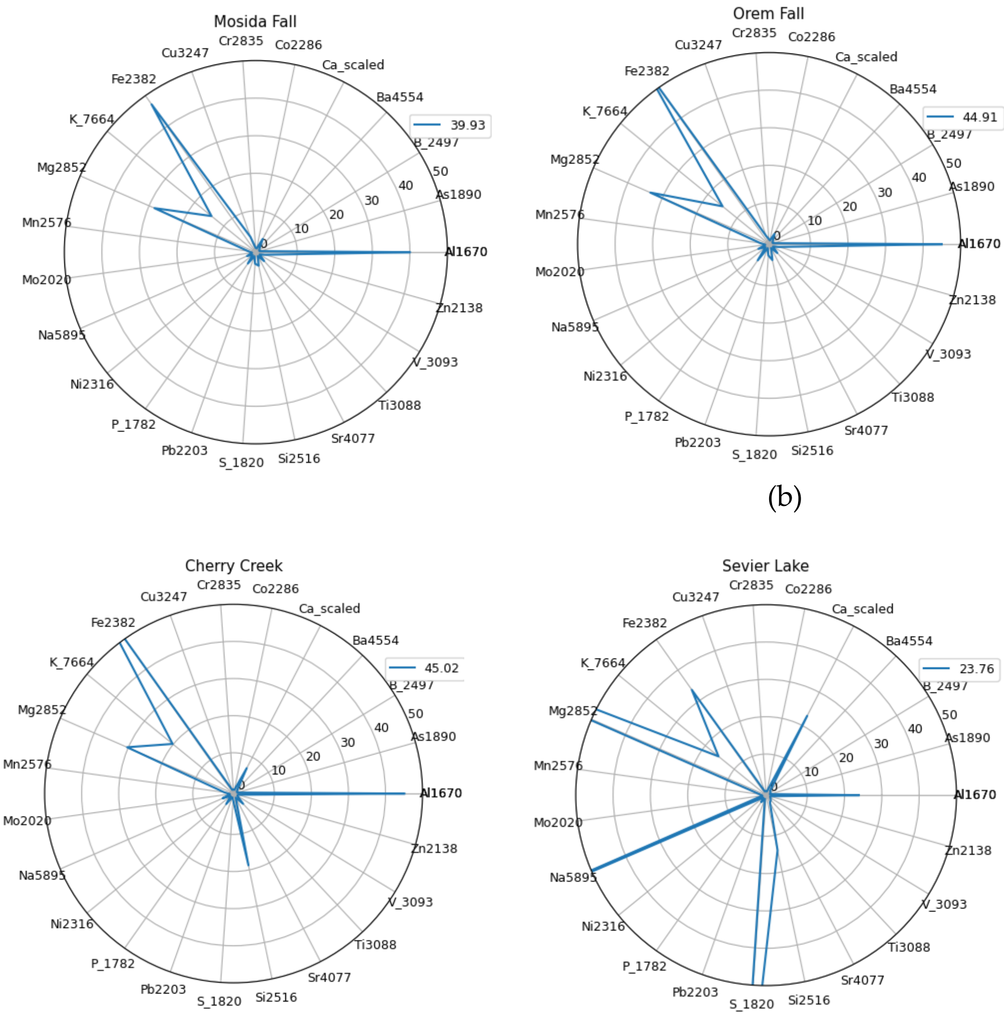

(b)

(c)

(d)

The time period of this study was during the high dust production for the area, in the months before and after the study the area is often wet or snowy, preventing local dust generation. This low level of collected dust strongly suggests that dust is not the primary source of nutrient loading to Utah Lake. These dust measurements support the research by Brahney [8] and Carling showing low levels of nutrients when looking at dry deposition alone. This is likely due to dust deposition consisting of larger settleable particulates compared to bulk deposition containing non-settling particulates. Bulk deposition is able to wash the $PM_{2.5}$ fraction, containing higher phosphorus levels [19], that are not collected efficiently in dry deposition sampling.

Table 1. Weights of dust collected over the course of 5.5 months for this study.

Location	Dust Collected (grams)		Total Dust (grams)
Mosida Fall	0.05	Mosida Total	0.12
Mosida Spring	0.07	Lake Shore Total	0.22
Lake Shore Fall	0.11	Pump Station Total	0.23
Lake Shore Spring	0.11	Orem Total	0.12
Pump Station Fall	0.03	Bird Island Total	0.05
Pump Station Spring	0.16		
Pump Station Contamination	0.04		
Orem Fall	0.05		
Orem Spring	0.07		
Bird Island Total	0.05		
Bird Island subtracting last sample	0.02		

The Utah Lake Science Panel has also debated whether nutrient deposition on the middle of the lake is similar to the shoreline. Barrus, Williams [21] placed the Bird Island sampler to try and determine the correct answer to this debate. Their results showed that the Bird Island sampler collected similar phosphorus levels to the shoreline samplers [21]. However, the panel claimed that the nutrients collected on Bird Island were likely due to contamination from birds or other sources. In unpublished internal science panel communications, a Student T test and Tukey-Kramer analysis were performed and showed that Bird Island's nutrient levels were not statistically different from the shoreline samplers. The tests from these internal memos are seen in Figure 9 and show that Bird Island is statistically similar to shoreline samplers while the no longer used Saratoga Springs sampler was the outlier. This similarity rules out contamination, as contamination would not have values consistent with the atmospheric deposition at the other sites. This statistical similarity supports the claim of Barrus, Williams [21] that nutrient deposition is similar mid-lake to the shoreline. The low levels of dust we collected combined with results shown by Brahney [8] suggest that dry deposition is a very small source of nutrient loading compared to bulk (precipitation) deposition measured by Miller.

The dust weights collected also provide insight into how dust deposition is changing across the lake. The Orem and Mosida samplers are on opposite sides of the lake and collected nearly identical amounts of dust. The MDS plot in Figure 6 shows a close similarity between the dusts collected at the Orem and Mosida samplers. The similar weight and composition of the two samples suggests that deposition is not changing significantly across the lake. However, the Bird Island sampler is located close to the path between Mosida and Orem but collected far less dust. Several of the samples from Bird Island showed zero or near zero dust collected for the week while the last week of collection more than doubled the dust collected. These weight differences may be caused by Bird Islands proximity to West Mountain. It is possible that the mountain is channeling the winds in a way that misses Bird Island while still crossing from Mosida to Orem.

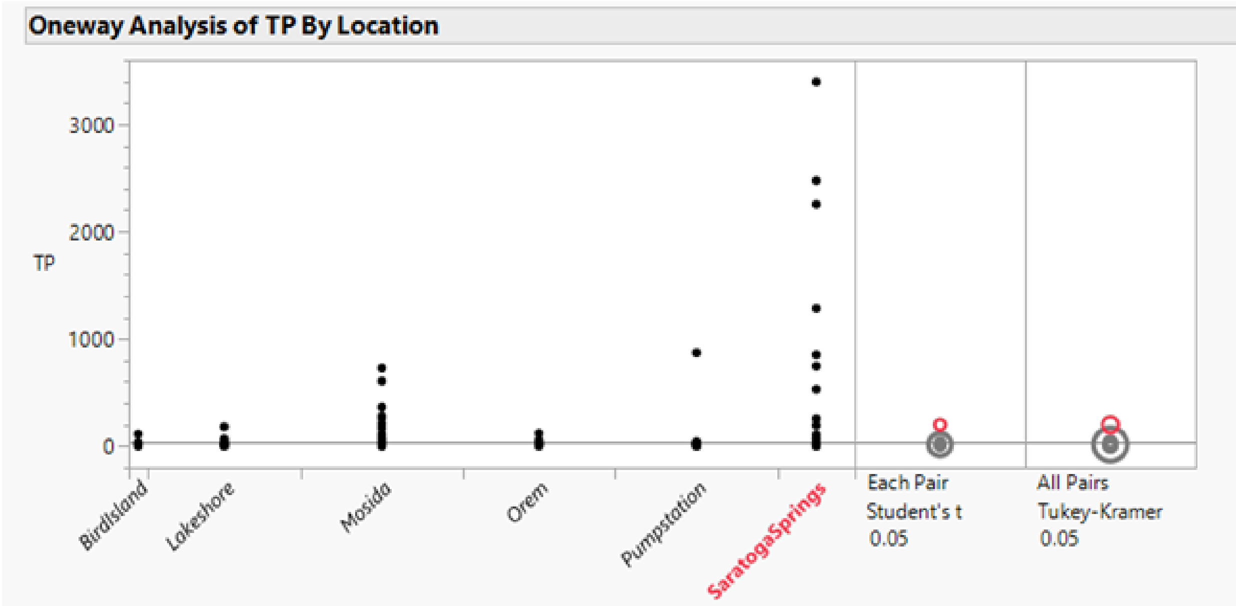

Figure 9. The results from a student T-test and a Tukey-Kramer test. The plot at the right shows that only Saratoga Springs is an outlier. The red circle represents Saratoga Springs. The grey circle represents all the remaining sites for both tests. There is no significant statistical difference at the p=0.05 level from Bird Island and any of the other sites.

4 Conclusion

The majority of dust deposition on Utah Lake comes from local fields south and west of the lake. Looking at the MDS plot and spectral angles shows that the most similar source location to all the deposition samples is Cherry Creek closely followed by Chimney Rock Pass. The previously suggested distant desert playa sources likely still contribute to deposition but contribute less than local areas. The two Lake Shore Samplers share the least similarity to the local sources and the strongest similarity to the desert playas of all the deposition samples. This is likely due to the sampler's close proximity to West Mountain, which blocks local transport from Cherry Creek but not long range transport from the desert playas. The major source to these two samplers was not found and more testing would be needed to fully understand what is happening.

Dust deposition is likely a minor source of the nutrient loading onto Utah Lake. This is shown by the research of Brahney [8] and carling looking at dust deposition and finding small nutrient loads compared to Miller and Barrus, Williams [21] who looked at bulk and total deposition. We also see evidence of dust being a minor contributor when comparing the dust weights collected to the similar nutrient loadings found by Barrus, Williams [21] between Bird Island and shoreline samplers. Dust cannot be the main source of nitrogen and phosphorus when there is no dust collected but nutrients are still present. The Utah Lake Science Panel internal communications provide statistics showing that these nutrients are not likely to have been caused by contamination of the samples.

Dust deposition across Utah Lake appears to be relatively unchanged as you travel away from the shoreline as has been suggested. We see this when looking at the amounts of dust and the similar elemental makeup of the Orem and Mosida samples. Both Orem and Mosida have major sources from Cherry Creek and Chimney Rock Pass. The Mosida sampler is on the same side of the lake as these sources while Orem is on the far side of the lake. The near identical dust weights and similar source compositions suggest that the dust concentrations are not changing across the lake as previously suggested. The Bird Island sampler is located just south of the path between Orem and Mosida and collected similar dust compositions but far less dust. This may be due to Bird Islands proximity to West Mountain, which may affect wind patterns and shield the island to some degree.

References

1. Merritt, L. and A. Miller, Interim Report on Nutrient Loadings to Utah Lake. Report to the Utah Department of Water Quality: Salt Lake City, UT, USA, 2016.
2. Randall, M.C., et al., Sediment potentially controls in-lake phosphorus cycling and harmful cyanobacteria in shallow, eutrophic Utah Lake. PloS one, 2019. 14(2): p. e0212238.
3. Olsen, J.M., et al., Measuring and calculating current atmospheric phosphorous and nitrogen loadings to Utah Lake using field samples and geostatistical analysis. Hydrology, 2018. 5(3): p. 45.
4. Zheng, T., et al., Characteristics of Atmospheric Deposition during the period of algal bloom formation in urban water bodies. Sustainability, 2019. 11(6): p. 1703.
5. Tanner, K.B., A.C. Cardall, and G.P. Williams. Analysis of long-term chlorophyll trends in Utah Lake using Landsat Data and Lake Regions. in 2022 Intermountain Engineering, Technology and Computing (IETC). 2022. IEEE.
6. Hansen, C.H., et al., Spatiotemporal variability of lake water quality in the context of remote sensing models. Remote Sensing, 2017. 9(5): p. 409.
7. Hansen, C.H., et al., Evaluating historical trends and influences of meteorological and seasonal climate conditions on lake chlorophyll a using remote sensing. Lake and Reservoir Management, 2020. 36(1): p. 45-63.
8. Brahney, J., Estimating total and bioavailable nutrient loading to Utah Lake from the atmosphere. 2019.
9. Brahney, J., et al., Increasing Ca2+ deposition in the western US: The role of mineral aerosols. Aeolian Research, 2013. 10: p. 77-87.
10. Clow, D.W., M.W. Williams, and P.F. Schuster, Increasing aeolian dust deposition to snowpacks in the Rocky Mountains inferred from snowpack, wet deposition, and aerosol chemistry. Atmospheric Environment, 2016. 146: p. 183-194.
11. Mahowald, N.M., et al., Aerosol Deposition Impacts on Land and Ocean Carbon Cycles. Current Climate Change Reports, 2017. 3(1): p. 16-31.
12. Belnap, J. and D.A. Gillette, Vulnerability of desert biological soil crusts to wind erosion: the influences of crust development, soil texture, and disturbance. Journal of arid environments, 1998. 39(2): p. 133-142.
13. Anderson, K.A. and J.A. Downing, Dry and wet atmospheric deposition of nitrogen, phosphorus and silicon in an agricultural region. Water, Air, and Soil Pollution, 2006. 176(1): p. 351-374.
14. Goudie, A.S., Dust storms: Recent developments. Journal of environmental management, 2009. 90(1): p. 89-94.
15. Prospero, J.M., et al., Environmental characterization of global sources of atmospheric soil dust identified with the Nimbus 7 Total Ozone Mapping Spectrometer (TOMS) absorbing aerosol product. Reviews of geophysics, 2002. 40(1): p. 2-1-2-31.
16. Skiles, S.M., et al., Implications of a shrinking Great Salt Lake for dust on snow deposition in the Wasatch Mountains, UT, as informed by a source to sink case study from the 13–14 April 2017 dust event. Environmental Research Letters, 2018. 13(12): p. 124031.

17. Abbott, B.W., et al., Emergency measures needed to rescue Great Salt Lake from ongoing collapse.

18. Hinds, W.C. and Y. Zhu, Aerosol technology: properties, behavior, and measurement of airborne particles. 2022: John Wiley & Sons.

19. Aarons, S.M., et al., Geochemical characterization of critical dust source regions in the American West. Geochimica et Cosmochimica Acta, 2017. 215: p. 141-161.

20. Abu-Hmeidan, H.Y., G.P. Williams, and A.W. Miller, Characterizing total phosphorus in current and geologic Utah Lake sediments: Implications for water quality management issues. Hydrology, 2018. 5(1): p. 8.

21. Barrus, S.M., et al., Nutrient Atmospheric Deposition on Utah Lake: A Comparison of Sampling and Analytical Methods. Hydrology, 2021. 8(3): p. 123.

22. Reidhead, J.G., Significance of the Rates of Atmospheric Deposition Around Utah Lake and Phosphorus-Fractionation of Local Soils. 2019.

23. Sickman, J.O., J.M. Melack, and D.W. Clow, Evidence for nutrient enrichment of high-elevation lakes in the Sierra Nevada, California. Limnology and Oceanography, 2003. 48(5): p. 1885-1892.

24. Morales-Baquero, R., E. Pulido-Villena, and I. Reche, Atmospheric inputs of phosphorus and nitrogen to the southwest Mediterranean region: Biogeochemical responses of high mountain lakes. Limnology and Oceanography, 2006. 51(2): p. 830-837.

25. Pulido-Villena, E., I. Reche, and R. Morales-Baquero, Evidence of an atmospheric forcing on bacterioplankton and phytoplankton dynamics in a high mountain lake. Aquatic sciences, 2008. 70(1): p. 1-9.

26. Maughan, E.K., Phosphoria Formation (Permian) and its resource significance in the western interior, USA. 1994.

27. Carling, G.T., et al., Using strontium isotopes to trace dust from a drying Great Salt Lake to adjacent urban areas and mountain snowpack. Environmental Research Letters, 2020. 15(11): p. 114035.

28. Goodman, M.M., et al., Trace element chemistry of atmospheric deposition along the Wasatch Front (Utah, USA) reflects regional playa dust and local urban aerosols. Chemical Geology, 2019. 530: p. 119317.

29. Lawrence, C.R. and J.C. Neff, The contemporary physical and chemical flux of aeolian dust: A synthesis of direct measurements of dust deposition. Chemical Geology, 2009. 267(1-2): p. 46-63.

30. NADP, NADP Site Selection and Installation Manual. 2022, Wisconsin State Laboratory of Hygiene.

31. Wang, X., et al., Surface sample collection and dust source analysis in northwestern China. Catena, 2005. 59(1): p. 35-53.

32. Ashbaugh, L.L., et al., Soil sample collection and analysis for the fugitive dust characterization study. Atmospheric Environment, 2003. 37(9-10): p. 1163-1173.

33. Dansie, A., et al., Measurements of windblown dust characteristics and ocean fertilization potential: The ephemeral river valleys of Namibia. Aeolian research, 2017. 29: p. 30-41.

34. Chepil, W., Sedimentary Characteristics of Dust Stos, III. Composition of Suspended Dust. Amer I, Sci, 1957. 255: p. 206.

35. Péwé, T.L., An observation on wind-blown silt. The Journal of Geology, 1951. 59(4): p. 399-401.

36. Kleiner, J., Coprecipitation of phosphate with calcite in lake water: a laboratory experiment modelling phosphorus removal with calcite in Lake Constance. Water Research, 1988. 22(10): p. 1259-1265.

37. Saleh, M., et al., Application of statistical analyses for lapis lazuli stone provenance determination by XRL and XRF. Microchemical Journal, 2020. 154: p. 104655.

38. Roberts, W., et al., Hydrostats: A Python package for characterizing errors between observed and predicted time series. Hydrology, 2018. 5(4): p. 66.

39. Vermeesch, P., Multi-sample comparison of detrital age distributions. Chemical Geology, 2013. 341: p. 140-146.

40. Vermeesch, P. and E. Garzanti, Making geological sense of 'Big Data'in sedimentary provenance analysis. Chemical Geology, 2015. 409: p. 20-27.

41. Kruskal, J.B., Multidimensional scaling by optimizing goodness of fit to a nonmetric hypothesis. Psychometrika, 1964. 29(1): p. 1-27.

Radar Plots

Source Dirt Radar Plots

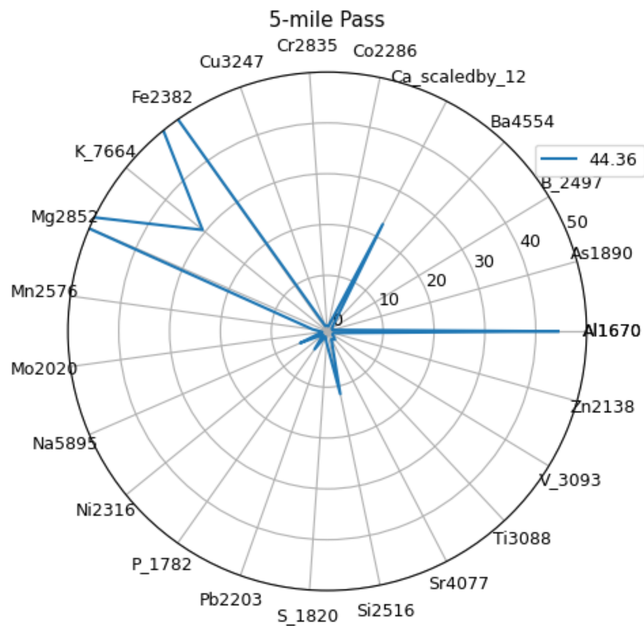

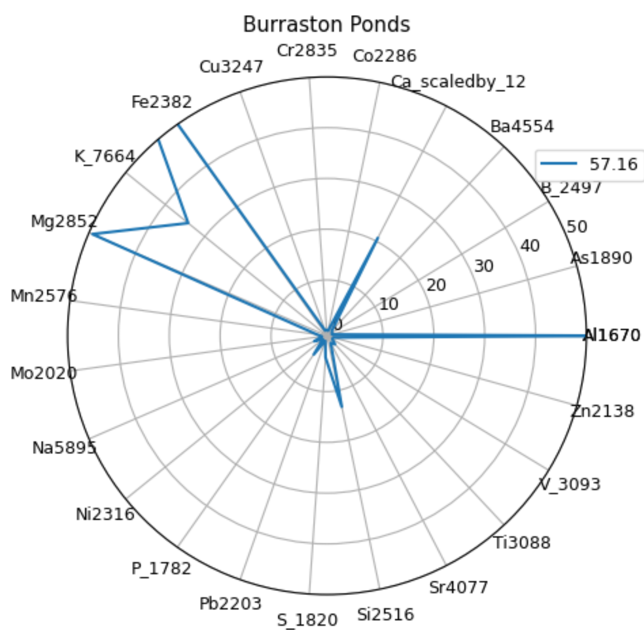

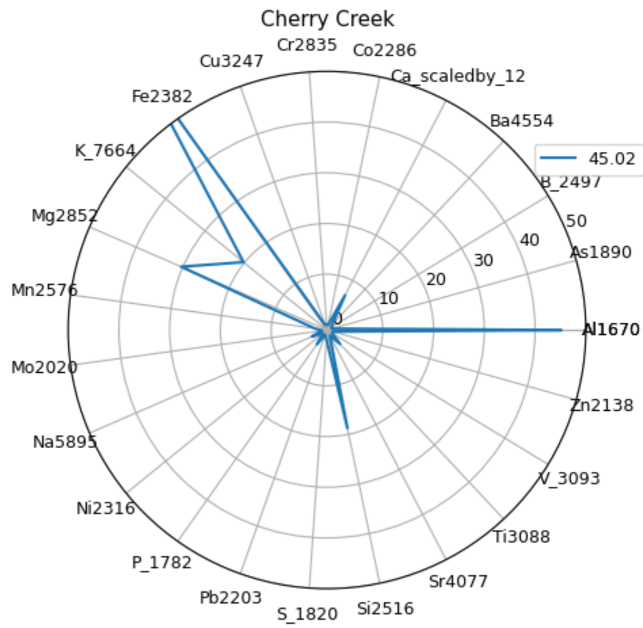
Cherry Creek
Cr2835
Co2286
Ca_scaledby_12
Ba4554
B_2497
As1890
Al1670
Zn2138
V_3093
Ti3088
Sr4077
Si2516
S_1820
Pb2203
P_1782
Ni2316
Na5895
Mo2020
Mn2576
Mg2852
K_7664
Fe2382
Cu3247
0
10
20
30
40
50
45.02

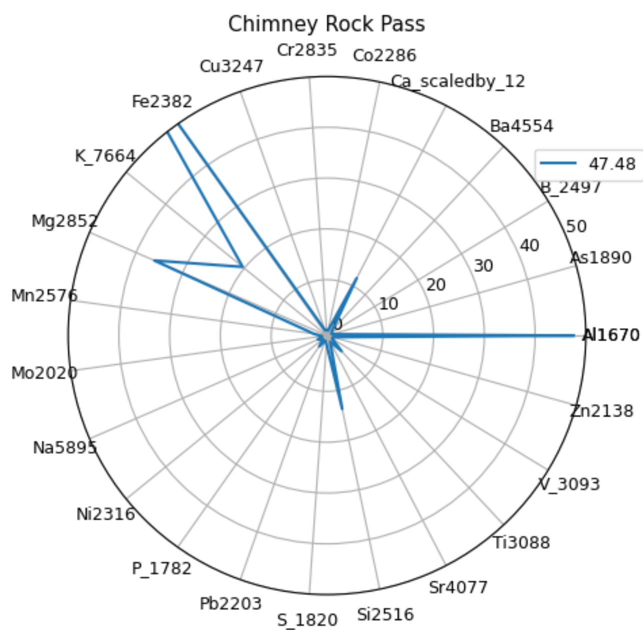
Chimney Rock Pass
Cr2835
Co2286
Ca_scaledby_12
Ba4554
B_2497
As1890
Al1670
Zn2138
V_3093
Ti3088
Sr4077
Si2516
S_1820
Pb2203
P_1782
Ni2316
Na5895
Mo2020
Mn2576
Mg2852
K_7664
Fe2382
Cu3247
0
10
20
30
40
50
47.48

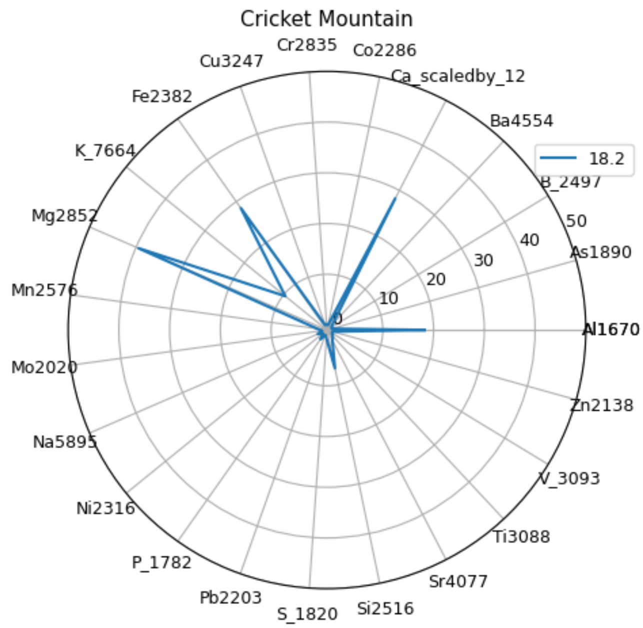
Cricket Mountain
Cr2835
Co2286
Ca_scaledby_12
Ba4554
B_2497
As1890
Al1670
Zn2138
V_3093
Ti3088
Sr4077
Si2516
S_1820
Pb2203
P_1782
Ni2316
Na5895
Mo2020
Mn2576
Mg2852
K_7664
Fe2382
Cu3247
0
10
20
30
40
50
18.2

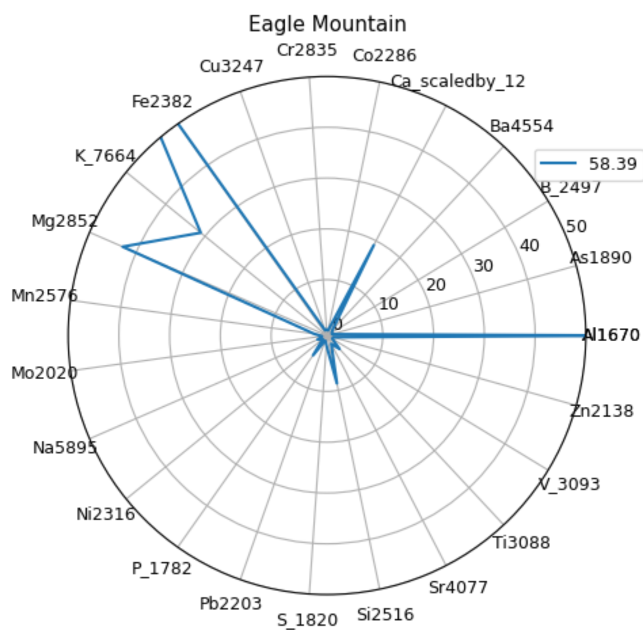
Eagle Mountain
Cr2835
Co2286
Ca_scaledby_12
Ba4554
B_2497
As1890
Al1670
Zn2138
V_3093
Ti3088
Sr4077
Si2516
S_1820
Pb2203
P_1782
Ni2316
Na5895
Mo2020
Mn2576
Mg2852
K_7664
Fe2382
Cu3247
0
10
20
30
40
50
58.39

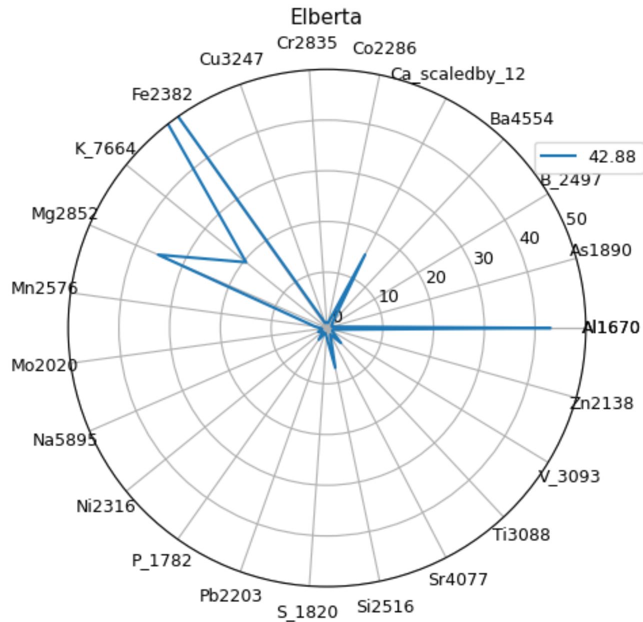
Elberta
42.88
Al1670
As1890
B_2497
Ba4554
Ca_scaledby_12
Co2286
Cr2835
Cu3247
Fe2382
K_7664
Mg2852
Mn2576
Mo2020
Na5895
Ni2316
P_1782
Pb2203
S_1820
Si2516
Sr4077
Ti3088
V_3093
Zn2138
0
10
20
30
40
50

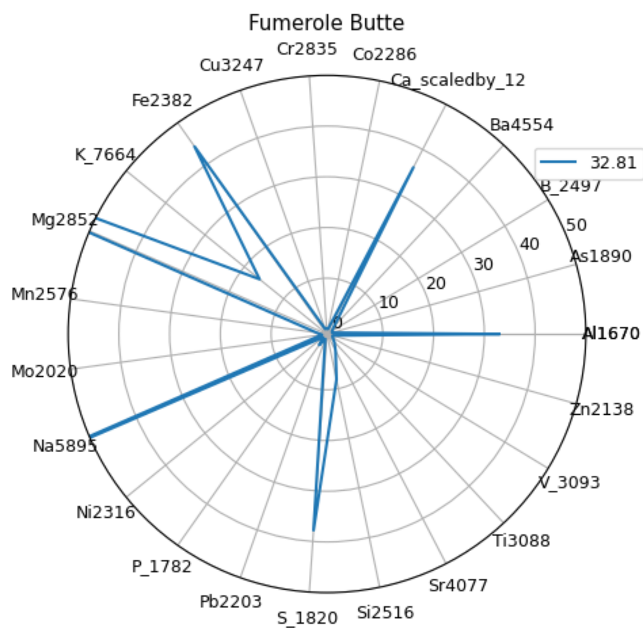
Fumerole Butte
32.81
Al1670
As1890
B_2497
Ba4554
Ca_scaledby_12
Co2286
Cr2835
Cu3247
Fe2382
K_7664
Mg2852
Mn2576
Mo2020
Na5895
Ni2316
P_1782
Pb2203
S_1820
Si2516
Sr4077
Ti3088
V_3093
Zn2138
0
10
20
30
40
50

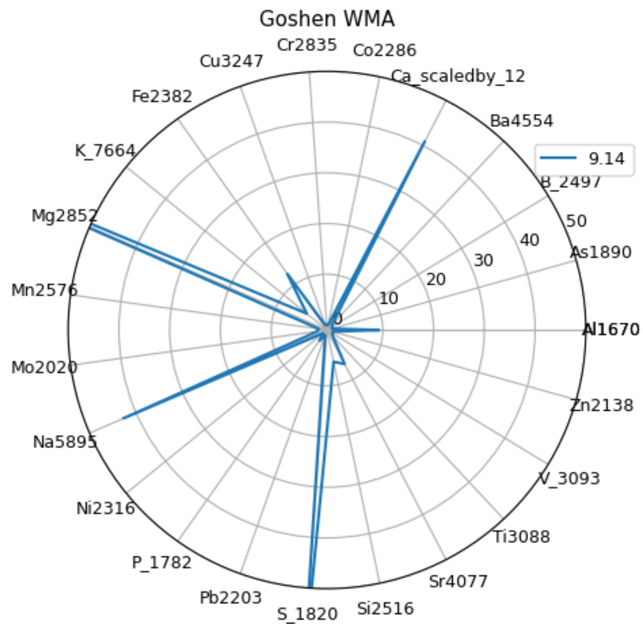
Goshen WMA
Cr2835
Co2286
Ca_scaledby_12
Ba4554
B_2497
As1890
Al1670
Zn2138
V_3093
Ti3088
Sr4077
Si2516
S_1820
Pb2203
P_1782
Ni2316
Na5895
Mo2020
Mn2576
Mg2852
K_7664
Fe2382
Cu3247
0
10
20
30
40
50
9.14

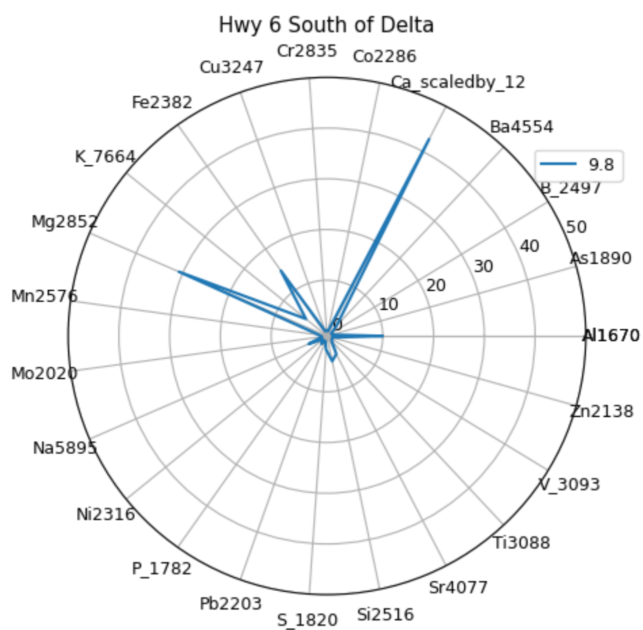
Hwy 6 South of Delta
Cr2835
Co2286
Ca_scaledby_12
Ba4554
B_2497
As1890
Al1670
Zn2138
V_3093
Ti3088
Sr4077
Si2516
S_1820
Pb2203
P_1782
Ni2316
Na5895
Mo2020
Mn2576
Mg2852
K_7664
Fe2382
Cu3247
0
10
20
30
40
50
9.8

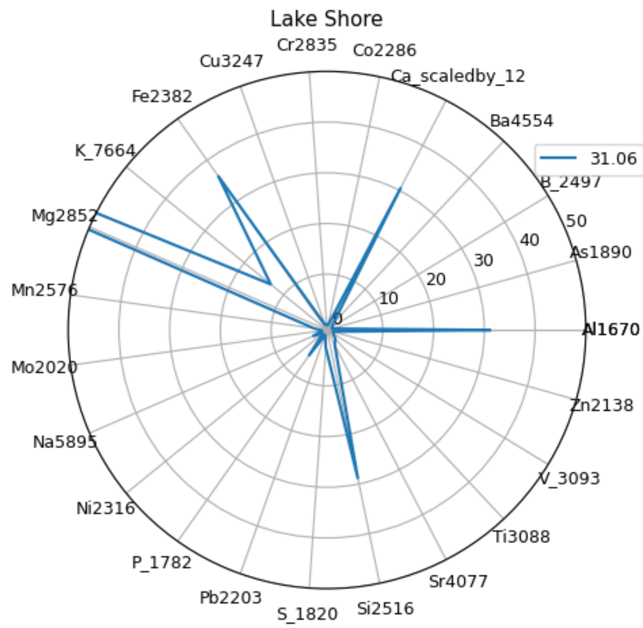
Lake Shore
Cr2835
Co2286
Ca_scaledby_12
Ba4554
B_2497
As1890
Al1670
Zn2138
V_3093
Ti3088
Sr4077
Si2516
S_1820
Pb2203
P_1782
Ni2316
Na5895
Mo2020
Mn2576
Mg2852
K_7664
Fe2382
Cu3247
0
10
20
30
40
50
31.06

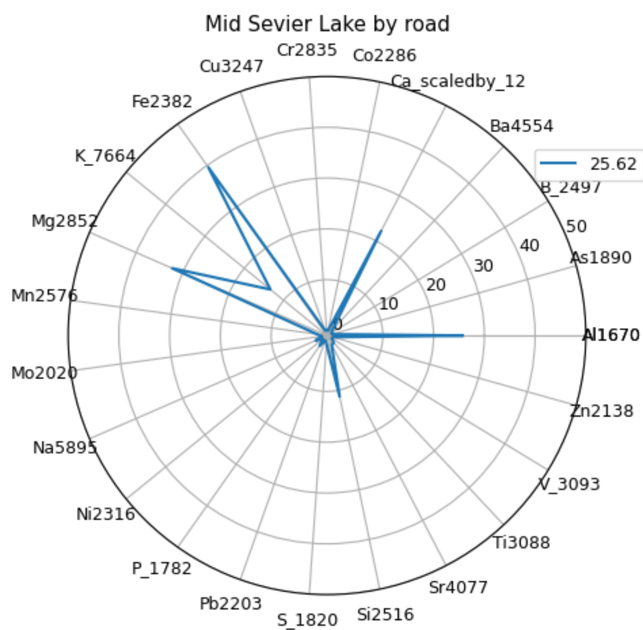
Mid Sevier Lake by road
Cr2835
Co2286
Ca_scaledby_12
Ba4554
B_2497
As1890
Al1670
Zn2138
V_3093
Ti3088
Sr4077
Si2516
S_1820
Pb2203
P_1782
Ni2316
Na5895
Mo2020
Mn2576
Mg2852
K_7664
Fe2382
Cu3247
0
10
20
30
40
50
25.62

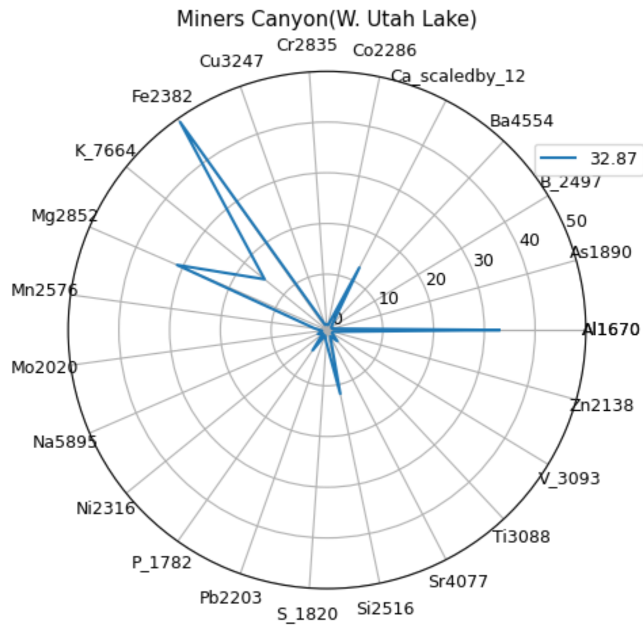
Miners Canyon(W. Utah Lake)
Cr2835
Co2286
Ca_scaledby_12
Ba4554
B_2497
As1890
Al1670
Zn2138
V_3093
Ti3088
Sr4077
Si2516
S_1820
Pb2203
P_1782
Ni2316
Na5895
Mo2020
Mn2576
Mg2852
K_7664
Fe2382
Cu3247
0
10
20
30
40
50
32.87

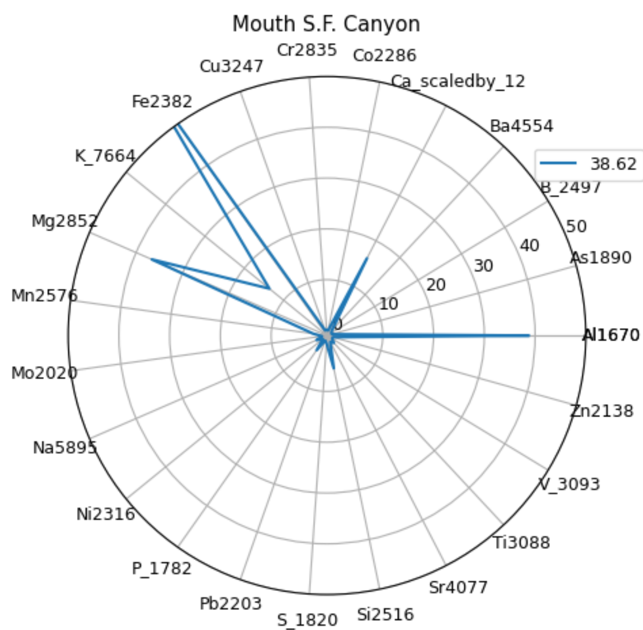
Mouth S.F. Canyon
Cr2835
Co2286
Ca_scaledby_12
Ba4554
B_2497
As1890
Al1670
Zn2138
V_3093
Ti3088
Sr4077
Si2516
S_1820
Pb2203
P_1782
Ni2316
Na5895
Mo2020
Mn2576
Mg2852
K_7664
Fe2382
Cu3247
0
10
20
30
40
50
38.62

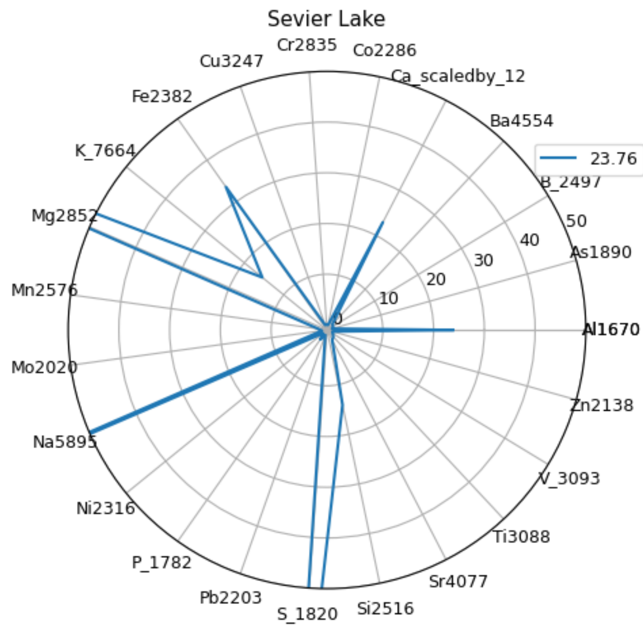
Sevier Lake
Cr2835
Co2286
Ca_scaledby_12
Ba4554
B_2497
As1890
Al1670
Zn2138
V_3093
Ti3088
Sr4077
Si2516
S_1820
Pb2203
P_1782
Ni2316
Na5895
Mo2020
Mn2576
Mg2852
K_7664
Fe2382
Cu3247
0
10
20
30
40
50
23.76

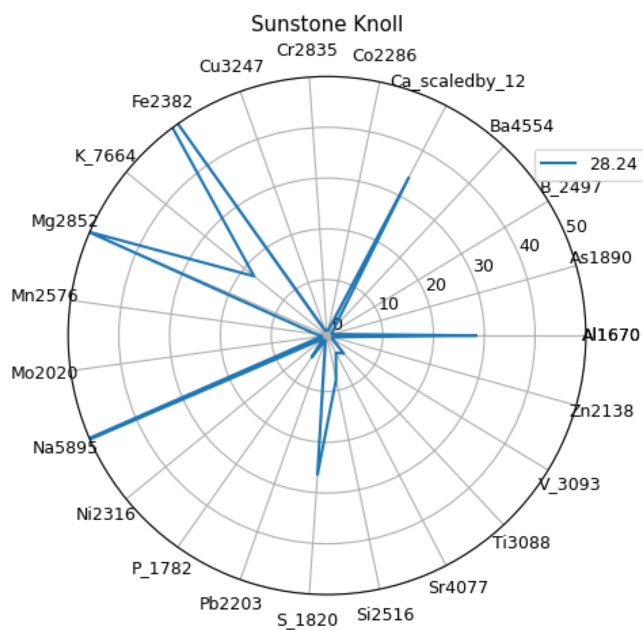
Sunstone Knoll
Cr2835
Co2286
Ca_scaledby_12
Ba4554
B_2497
As1890
Al1670
Zn2138
V_3093
Ti3088
Sr4077
Si2516
S_1820
Pb2203
P_1782
Ni2316
Na5895
Mo2020
Mn2576
Mg2852
K_7664
Fe2382
Cu3247
0
10
20
30
40
50
28.24

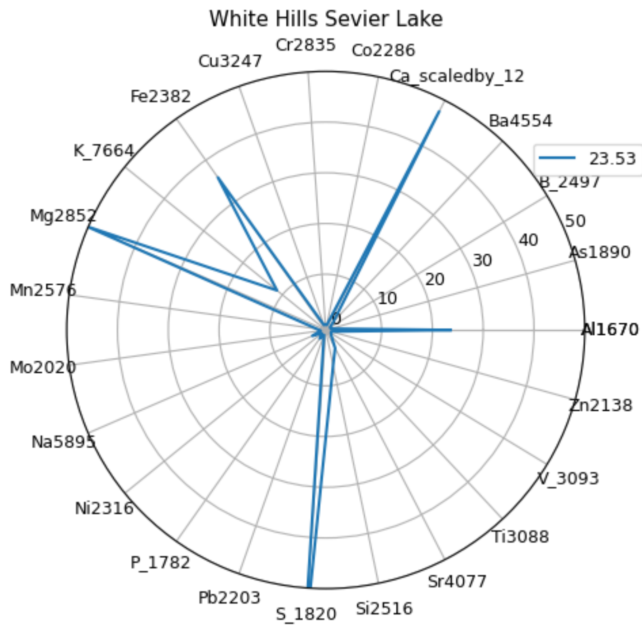

Deposition Sample Radar Plots

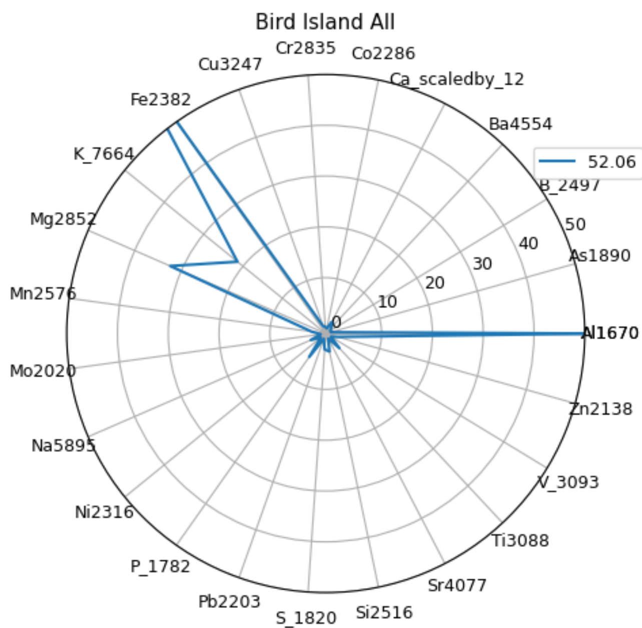

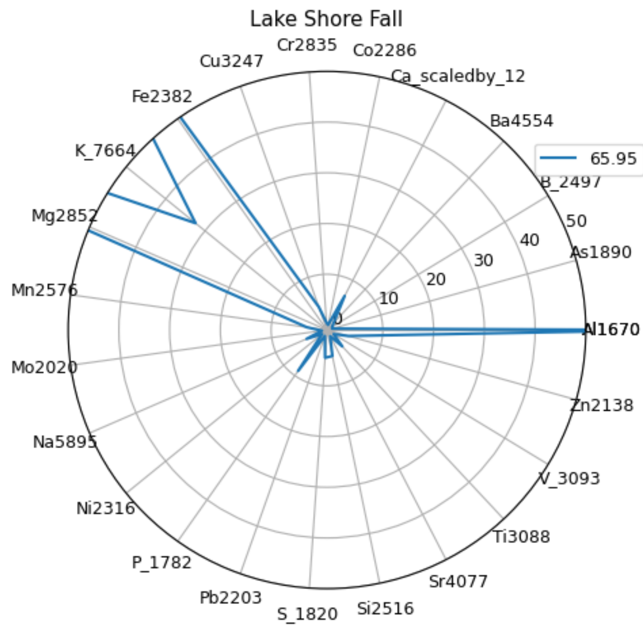
Lake Shore Fall
Cr2835
Co2286
Ca_scaledby_12
Ba4554
B_2497
As1890
Al1670
Zn2138
V_3093
Ti3088
Sr4077
Si2516
S_1820
Pb2203
P_1782
Ni2316
Na5895
Mo2020
Mn2576
Mg2852
K_7664
Fe2382
Cu3247
65.95
0
10
20
30
40
50

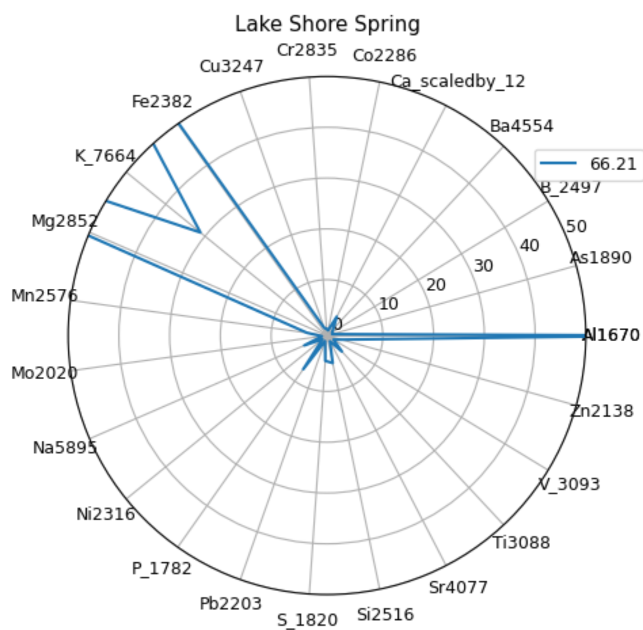
Lake Shore Spring
Cr2835
Co2286
Ca_scaledby_12
Ba4554
B_2497
As1890
Al1670
Zn2138
V_3093
Ti3088
Sr4077
Si2516
S_1820
Pb2203
P_1782
Ni2316
Na5895
Mo2020
Mn2576
Mg2852
K_7664
Fe2382
Cu3247
66.21
0
10
20
30
40
50

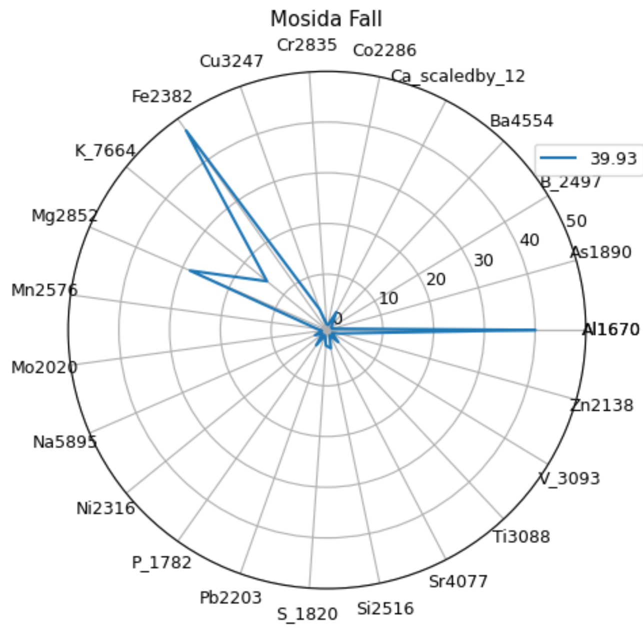

Mosida Fall
Cr2835
Co2286
Ca_scaledby_12
Ba4554
B_2497
As1890
Al1670
Zn2138
V_3093
Ti3088
Sr4077
Si2516
S_1820
Pb2203
P_1782
Ni2316
Na5895
Mo2020
Mn2576
Mg2852
K_7664
Fe2382
Cu3247
39.93
0
10
20
30
40
50

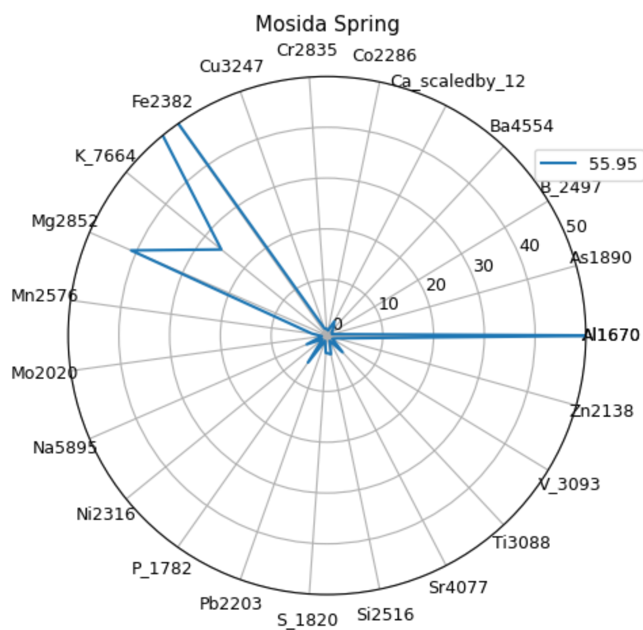

Mosida Spring
Cr2835
Co2286
Ca_scaledby_12
Ba4554
B_2497
As1890
Al1670
Zn2138
V_3093
Ti3088
Sr4077
Si2516
S_1820
Pb2203
P_1782
Ni2316
Na5895
Mo2020
Mn2576
Mg2852
K_7664
Fe2382
Cu3247
55.95
0
10
20
30
40
50

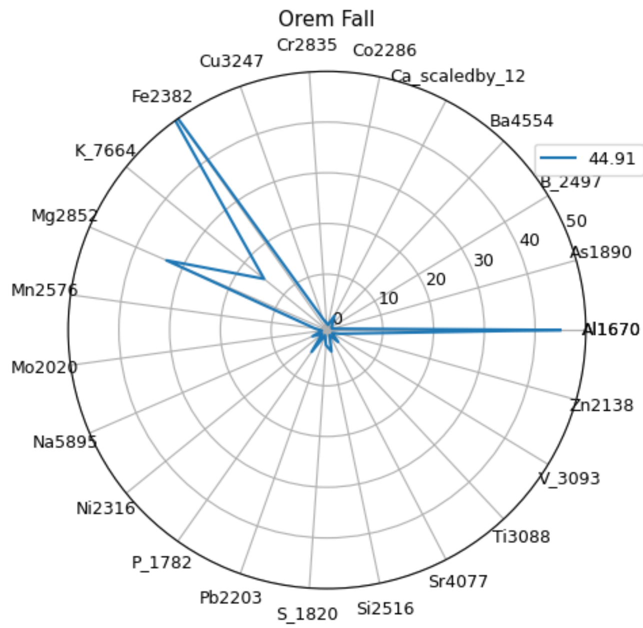
Orem Fall
Cr2835
Co2286
Ca_scaledby_12
Ba4554
B_2497
As1890
Al1670
Zn2138
V_3093
Ti3088
Sr4077
Si2516
S_1820
Pb2203
P_1782
Ni2316
Na5895
Mo2020
Mn2576
Mg2852
K_7664
Fe2382
Cu3247
44.91
0
10
20
30
40
50

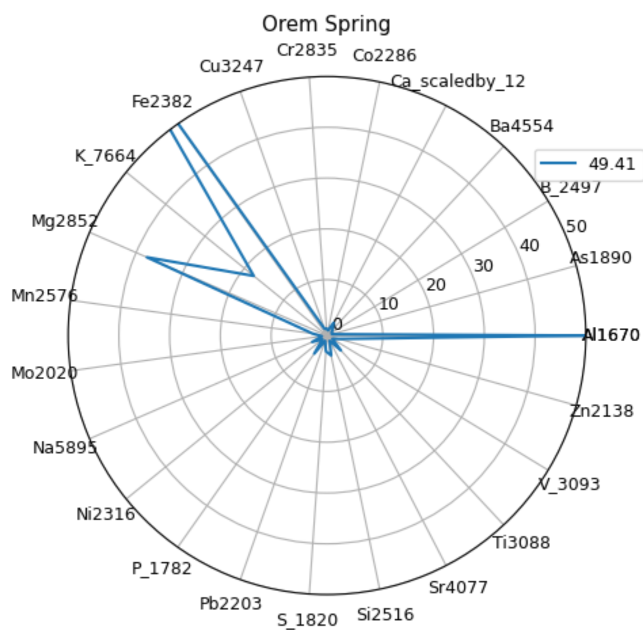
Orem Spring
Cr2835
Co2286
Ca_scaledby_12
Ba4554
B_2497
As1890
Al1670
Zn2138
V_3093
Ti3088
Sr4077
Si2516
S_1820
Pb2203
P_1782
Ni2316
Na5895
Mo2020
Mn2576
Mg2852
K_7664
Fe2382
Cu3247
49.41
0
10
20
30
40
50

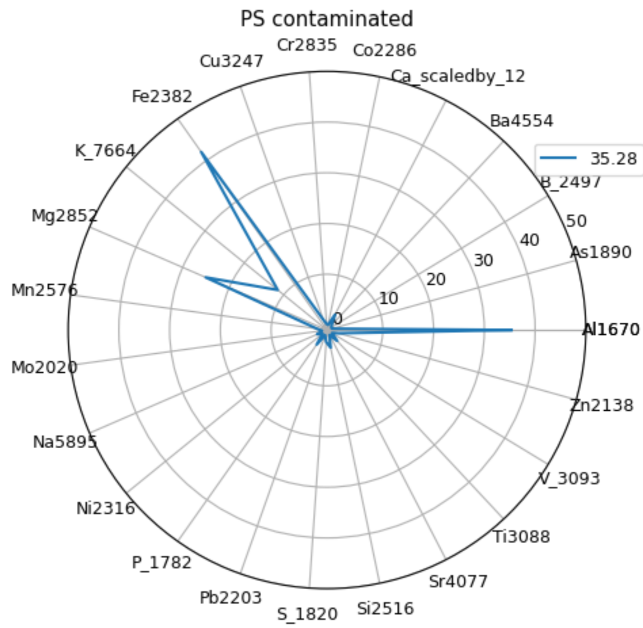
PS contaminated
Cr2835
Co2286
Ca_scaledby_12
Ba4554
B_2497
As1890
Al1670
Zn2138
V_3093
Ti3088
Sr4077
Si2516
S_1820
Pb2203
P_1782
Ni2316
Na5895
Mo2020
Mn2576
Mg2852
K_7664
Fe2382
Cu3247
0
10
20
30
40
50
35.28

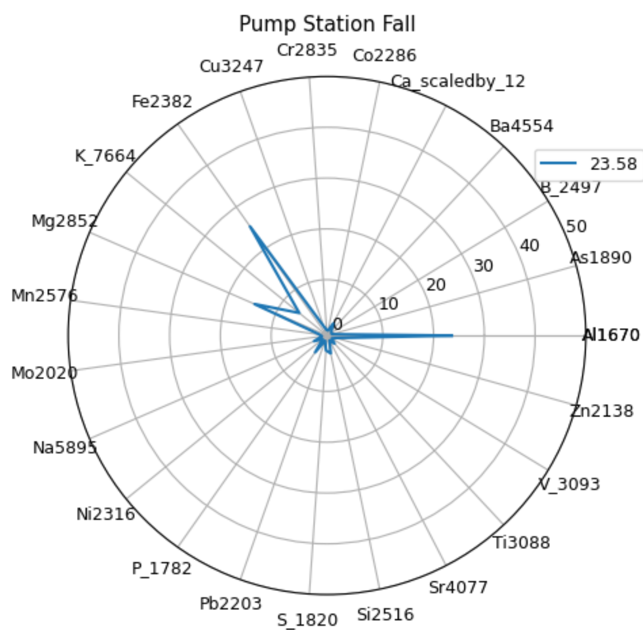
Pump Station Fall
Cr2835
Co2286
Ca_scaledby_12
Ba4554
B_2497
As1890
Al1670
Zn2138
V_3093
Ti3088
Sr4077
Si2516
S_1820
Pb2203
P_1782
Ni2316
Na5895
Mo2020
Mn2576
Mg2852
K_7664
Fe2382
Cu3247
0
10
20
30
40
50
23.58

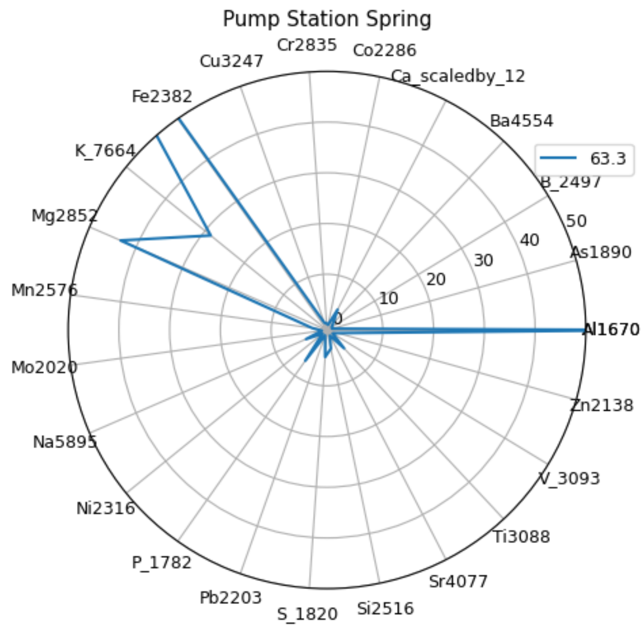
Pump Station Spring
Cr2835
Co2286
Ca_scaledby_12
Ba4554
B_2497
As1890
Al1670
Zn2138
V_3093
Ti3088
Sr4077
Si2516
S_1820
Pb2203
P_1782
Ni2316
Na5895
Mo2020
Mn2576
Mg2852
K_7664
Fe2382
Cu3247
63.3
0
10
20
30
40
50